Journal of Pharmacognosy and Phytochemistry
Available online at www.phytojournal.com

E-ISSN: 2278-4136
P-ISSN: 2349-8234
https://www.phytojournal.com
JPP 2024; 13(2): 662-669
Received: 22-02-2024
Accepted: 26-03-2024

Denni Mammen
School of Science, Navrachana University, Vasana-Bhaili Road, Vadodara, Gujarat, India

Deepak Malviya
School of Science, Navrachana University, Vasana-Bhaili Road, Vadodara, Gujarat, India

Parth Pandya
School of Science, Navrachana University, Vasana-Bhaili Road, Vadodara, Gujarat, India

Mammen Daniel
Dr. Daniel's Laboratories, Manjalpur, Vadodara, Gujarat, India

Corresponding Author:
Denni Mammen
School of Science, Navrachana University, Vasana-Bhaili Road, Vadodara, Gujarat, India

Identification features of *Vincetoxicum indicum*: Microscopy and DNA sequencing-based validation

Denni Mammen, Deepak Malviya, Parth Pandya and Mammen Daniel

DOI: https://doi.org/10.22271/phyto.2024.v13.i2d.14909

Abstract
Background: The present research work has been undertaken to identify key identification characters of *Vincetoxicum indicum*, a medicinal twiner with potency to expel mucus from the lungs. Leaf constants were calculated during micromorphological studies.
Methods: Transverse sections of leaf, stem and root were studied in detail to identify key characters that could help in proper identification of the plant. DNA was isolated from the plant in good purity and amplified using PCR, using RUBISCO gene as a phylogenetic marker. The gene was subjected to sequencing for identification of plant species, for which the sequences for both forward and reverse primers were obtained based on the electropherograms obtained.
Results: Uniseriate multicellular trichomes on both surfaces as well as sphaeraphides in ground tissue were important features in the leaf. Stem showed lignified metaxylem tracheids with ray cells. Sphaeraphides and sclereids were observed in the cortex, while starch grain laden parenchyma cells were observed in the pith region. Trichomes like those in leaf were also observed in the stem. The stele in root was tetrarch in nature, with large xylem vessels interspersed with tracheid elements. Cortex showed sphaeraphides and parenchyma with starch grains. The forward and reverse DNA sequences when uploaded to the NCBI BLAST database, showed similarity index above 99% which proved that the species is indeed *Vincetoxicum indicum*.
Conclusion: This work puts forth important microscopic features for proper identification of the plant, as well as species confirmation using DNA barcoding.

Keywords: *Vincetoxicum indicum*, micromorphology, transverse sections, DNA sequencing

Introduction
Vincetoxicum indicum (Burm. f.) Mabb., an important twining medicinal plant used for respiratory diseases to clear the lungs from the excess mucus. This plant, also synonymous with *Tylophora indica* (Burm. f.) Merr. And *Tylophora asthmatica* W. &A., has mucolytic and expectorant properties.
It may not help if the patient has a nonproductive asthmatic cough. Generally, most cases of asthma are nonproductive. Wheezing appears in them due to swelling and narrowing of the airways that occur due to the inflammatory response to triggers.
This medicinal herb is found in the central, eastern, and southern India, Thailand, Sri Lanka, Malaysia, and Borneo [1].

Fig 1: Whole plant, flowering, and fruiting stages of *Vincetoxicum indicum*

In-vivo analysis of leaf extract on rats showed good hepatoprotective effect [2]. Leaves were also found to be effective against 18 bacteria and 8 fungi [3-4]. Aerial parts reduced inflammation when tested on rats [5-6]. Roots of the plant showed significant antidiarrheal potential when tested on rats [7]. The leaves were proved to be hypolipidemic by decreasing total cholesterol, triglycerides, and low-density lipoprotein, while increasing the high-density lipoprotein in rats [8]. Alkaloids like tylophorine decreased the tumor size, as well as showed antiangiogenic activity in mice [9]. Leaf extract and isolated alkaloids of the plant showed significant anticancer activity against human ductal breast epithelial T47D cell line, human colon HCT-15 cell line, human liver Hep-G2 cell line, nasopharyngeal KB cell line, stomach carcinoma NUGC-3 cell line and epithelial HONE-1 cell line [10-13].

Materials and Methods

Fresh plant material was collected from Botanical Garden of The M.S. University of Baroda and compared with the Herbarium (BARO) in Department of Botany. Voucher specimen (D/1160) was deposited in Baroda University Herbarium.

Anatomy

Fresh leaf, stem and root portions of the plant were fixed in FAA [14]. They were embedded in paraffin and transverse sections were taken in a rotary microtome. Sections were selected and stained with safranin and after dehydration mounted in DPX and observed under microscope. Measurement of sizes (dimensions) of various cells and crystals and the photography were taken using CMOS 5.2-megapixel microscope camera with basic software (Medivizion Scientific Instruments, India). The quantitative data are based on an average of 50 readings.

Micromorphology

Fresh leaves were washed, and small fragments of leaves were taken from the middle region of the mature leaves. The washed leaf fragments were first boiled in 90% alcohol for about 3-5 minutes to remove chlorophyll, then washed 2-3 times with water, then boiled again with 10% KOH solution for 2-3 minutes and washed 4-5 times with water and were then kept in clean water to remove all traces of the clearing agent. The epidermal layer was peeled off with the help of a pointed needle and forceps. The epidermal peels were washed in water, stained with Safranin (0.5%) in water and then mounted in 50% glycerine; the margins of the coverslips were sealed with DPX. The slides were placed on top of another slide which had a permanent 1 mm x mm square on it.

Leaf constants such as stomatal index/ mm^2, trichome index/ mm^2, vein islet number/ mm^2, vein termination number/ mm^2, and palisade ratio were calculated. Each such quantitative data is a mean of 50 readings [15].

DNA isolation and sequencing

DNA was extracted using CTAB method by crushing fresh leaf sample in a mortar and pestle with buffer solution which is prepared by dissolving 100mM Tris HCl– (0.047g), 25mM EDTA (0.022 g), 2% CTAB (0.6 g), 1.5M NaCl (0.236 g), 5M NaCl (0.877g) and 0.3% β -Mercaptoethanol (0.1mL) in 30 mL water [16-19]. This treatment causes lysis of cell and DNA is exposed in the solution. The mixture is incubated in hot air oven at 60 °C for 10 minutes. The sample is shaken vigorously with chloroform and centrifuged at 4100 rpm for 15 minutes. The upper phase is transferred into another tube and treated with chloroform again. This step is repeated 3-4 times, treated with isopropanol, and centrifuged at 4000 rpm for 10 minutes. The supernatant is discarded, and the pellet remaining is vortexed after adding 3mL of 5M NaCl solution. To this, 7mL of ethyl alcohol is added, incubated at 0 °C for one hour, and centrifuged at 4000 rpm for 10 minutes. The alcohol layer is discarded and the pellet containing DNA is dissolved in 50 µL water and vortexed. The integrity of the extracted DNA was observed using agarose gel electrophoresis, in presence of ethidium bromide. The purity of the DNA was established by absorbance studies on Shimadzu 1900i UV-Vis spectrophotometer. The pure DNA was then further subjected to PCR amplification, where RUBISCO gene was used as a phylogenetic marker. DNA sequencing of the sample was outsourced from Eurofins Genomics India, Bengaluru. Sequences for both forward and reverse primers were obtained. Contig was made using Bioedit Bioinformatic software. The sequence obtained was subjected to NCBI BLAST, and the sequence was uploaded, and its similarity search was performed to confirm the species level identification.

Results

Micromorphology

The various leaf constants of *V. indicum* mature leaf calculated as shown in Table 1.

Table 1: Calculated leaf constants for *V. indicum* (*Each value is a mean of 50 readings)

Sr. No.	Leaf Constants	Quantitative Data*
1.	Stomatal Index	3.99 ± 0.52
2.	Trichome Index	2.99 ± 0.34
3.	Palisade ratio	3.07 ± 0.29
4.	Vein Islet Number	42.06 ± 0.41
5.	Vein Termination Number	1.98 ± 0.27

T.S. of leaf

The leaf is dorsiventral in nature with 2-3 layered palisade and 5-6 layers of spongy tissue (Figure 2C). Upper epidermis consists of barrel shaped cells having a breadth of about 65-75 µm and 12-14 µm in height. This is covered by a very thin cuticle. Upper palisade layer consists of vertically rectangular cells with height of 90-95 µm and 30-35 µm breadth. These cells contain 1 or 2 spherical chloroplasts having diameter 11-13 µm. Lower palisade layer is slightly shorter 70-80 µm in height and 30-35 µm broad. These cells contain 5-6 spherical chloroplasts. Mesophyll adjoining the palisade is spherical in shape with 1-2 chloroplasts. Middle spongy tissue consists of oval or elongated parenchyma (length 75-80 µm, breadth 25-30 µm) slightly extended parallel to the surface and contain very few chloroplasts.

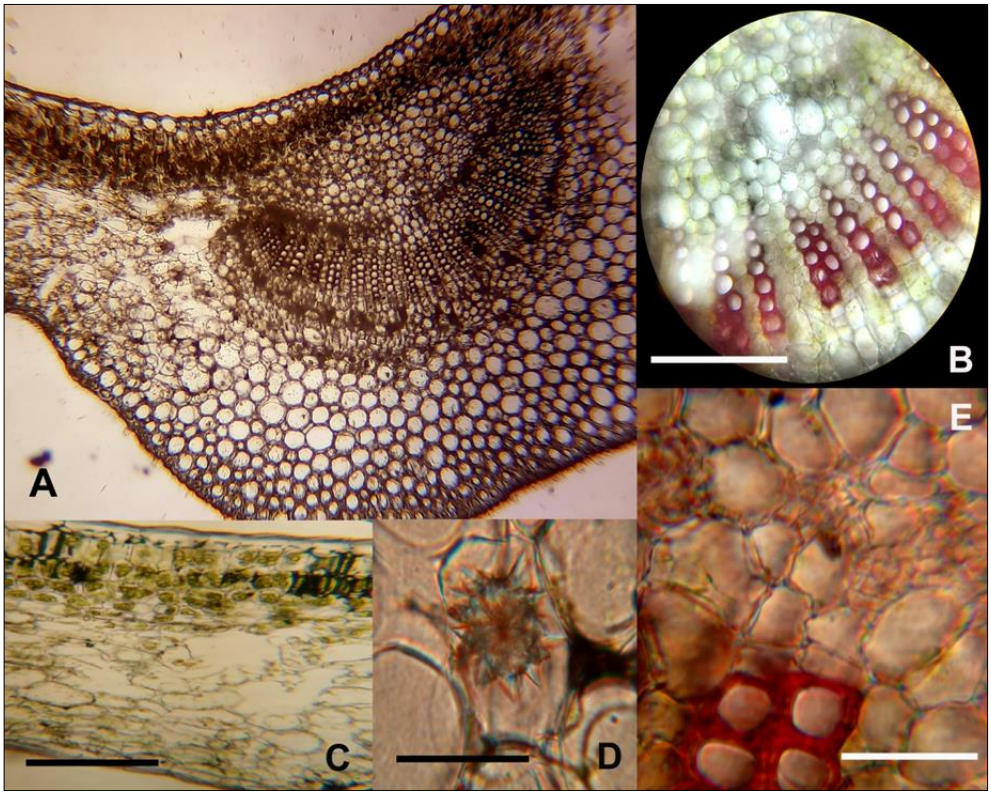

Fig 2: A. View of transverse section of leaf. B. Vertical rows of tracheids separated by medullary rays. C. Palisade and spongy tissue in lamina. D. Sphaeraphides in ground tissue parenchyma. E. Phloem elements along with xylem tracheids. Scale bar: 400 µ (B, C), and 100µ (D, E)

Lower epidermal cells are also barrel shaped but consisting of shorter cells with breadth 17-19 µm and height of 12-14 µm, with slightly sunken stomata and a thin cuticle. Uniseriate multicellular hairs were observed on both surfaces, with more of them on the lower epidermal surface. Each cell in the hair shows a length of 39-42 µm and breadth of 17-19 µm. The midrib region contained a single vascular bundle embedded in spongy tissue. The xylem contained mainly tracheids with metaxylem showing diameter of 16-18 µm. Vertical rows of tracheids were separated by medullary rays (Fig 2B). Phloem consisted of very small sieve tubes separated by wide medullary rays (Fig 2E). The palisade was continuous above vascular bundle (Fig 2A). The ground tissue below the vascular bundle were 8-10 cells broad and consists of closely packed spherical parenchyma containing an average diameter of 15-40 µm. Several isolated sphaeraphides were observed among the parencymatous tissue (Figure 2D).

T.S. of stem

The stem appeared elliptical in the T.S. due to the anomalous secondary growth of stem facilitating the twining habit. The elliptical young stem has a diameter of 3500-3700 µm at long plane and 2400-2600 µm breadth (Figure 3A). This pattern is due to the abnormal secondary thickening in which two patches of cambium on either side of stem produce very little xylem towards inside while producing many layers of phloem towards outside much like the wedge-shaped phloem as observed in *Bignonia*. This results in narrowing of the middle region and elliptical shape is observed. It is because, the habit of the plant being twining in nature, the less of secondary xylem which is a mechanical tissue in the central plane gives the stem flexibility to twist around a support.

The stem possesses a large stele (about 35%) enclosing a pith which amounts to about 25% and a comparatively large cortex. Primary xylem consists of a continuous ring of vertical rows of outer 4-6 metaxylem tracheids which are almost square in outline and inner 1-2 round protoxylem elements, separated by similar vertical rows of xylem rays. In contrast to other dicot stems there are no discrete vascular bundles (Fig 3A). Inner to primary xylem are internal phloem arranged in big or small groups (Fig 3C). Outer to primary xylem are the secondary vascular tissues. As mentioned in the beginning the secondary thickening is anomalous in nature due to abnormal activity of cambium. Except for two short patches on diagonally opposite sides, the cambium acts as usual producing xylem towards inside and phloem towards outside. The two aberrant patches of cambium produce little or no xylem (maybe one or two layers only) towards inside and continue to produce large amounts of phloem towards outside. This results in production of two large wedges of phloem jutting into xylem dividing the secondary xylem to two big patches on a plane at right angles to phloem wedges. The two secondary xylem groups appear lunar shaped and are oppositely placed. The secondary xylem consists of large vessels, sometimes two or three clubbed together tangentially. Vessels have an average diameter of 130-140 µm and are surrounded by very small tracheids having an average diameter of 10-14 µm. In the longitudinal section, each vessel segment is long (450-650 µm in length and 100-130 µm in breadth), has oblique end walls and contains 10-20 vertical rows of simple pits. The tracheids of primary xylem and of secondary xylem are quite different from each other. The former were larger having a diameter of 30 to 35 µm with a broad lumen, and a length of 650-1000 µm with transverse end walls. The tracheids of secondary xylem are smaller, having a diameter of 10-15 µm, with a very narrow lumen. Medullary rays are single celled or two cells in height, consisting of 50-55 µm high and 20-25 µm broad cells. The outer edges of secondary xylem are wavy. The two secondary xylem groups appear lunar shaped and are oppositely placed.

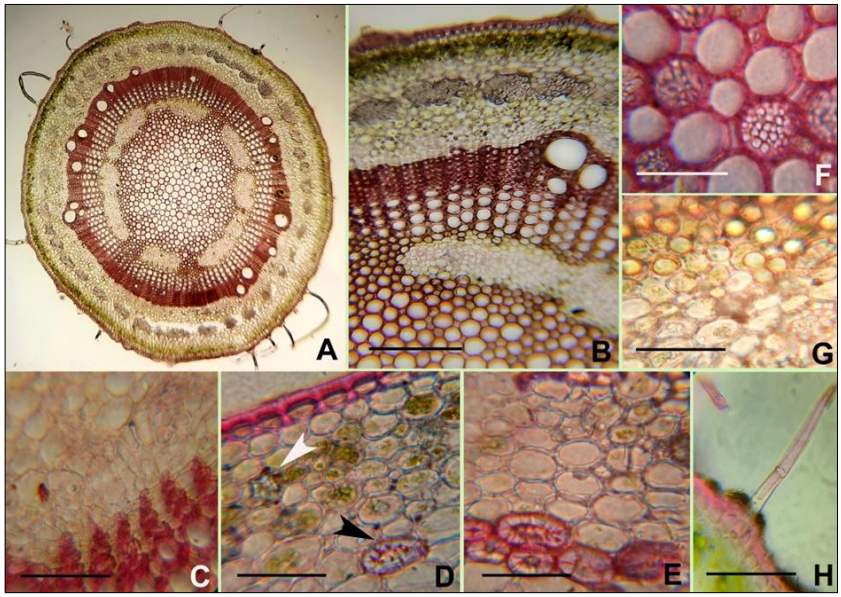

Fig 3: A. View of transverse section of stem B. Lignified metaxylem tracheids with ray cells. C. Phloem bundles along with tracheids. D. Cortex showing sphaeraphides (white arrow) and sclereids (black arrow). E. Rows of sclereids in the pericycle. F. Pith region with parenchyma full of starch grains. G. Oil glands. H. Uniseriate multicellular trichome. Scale bar: 400 µ (B), and 100µ (C-H)

Outer to secondary xylem, is a continuous patch of secondary phloem with crushed primary phloem pushed outside. Pericycle consists of an outer ring of sclereids, mostly singly in a peripheral line or in groups of 5-8 (Fig 3E), and an inner ring of sclerenchymatous patches (Fig 3E). Each sclereid is oval, pitted and 45-50 µm in breadth and 24-28 µm in height. The fibres are small, having very narrow lumen. Endodermis is not very clear. Cortex consists of 5-8 layers of chlorenchyma in the outside (Fig 3B, D). Cortical cells contain cluster crystals having diameter of 20-24µm (Figure 3D-white arrow). Hypodermis is of large chlorenchyma cells, having a breadth of 30-35 µm and a height of 15-18 µm. Epidermis consists of small rectangular cells 20-22 µm breadth and 10-13 µm in height covered by a 6-8µm thick cuticle. Epidermal hairs are multicellular uniseriate having a length of 120-130 µm in length and 12-15 µm in breadth (Figure 3H). Pith cells are parenchymatous with slight lignification, many filled with starch grains (Fig 3F).

T.S. of root

The roots are circular in cross section (Fig 4A) with a central stele encircled by a broad (in younger roots) or thin cortex (in older roots). The stele is tetrarch in nature.

The four protoxylem points get crushed in large secondary xylem but are visible if the four large xylem rays are traced to centre. There is a central large metaxylem element in centre. Secondary xylem consists of mostly radially arranged large vessels surrounded by tracheids (Fig 4F). The vessels may reach a diameter of 50 µm whereas the tracheids are small having a diameter of 8-10 µm. Central xylem is seen surrounded by broad patches of secondary phloem. Outer to phloem is a single layer of parenchymatous pericycle (Figure 4B). The outer most layer of stele, the endodermis, consists of barrel shaped cells (about 24 µm long and 12 µm broad) having thickening of yellow suberin on radial and outer tangential walls (Fig 4C). Cortex is uniform in having parenchyma cells rich in starch grains (Figure 4E) and a few sphaeraphides. The parenchyma cells are large and isodiametric in shape having a diameter of about 40 µm. Most of these cells are filled with many small circular starch grains having a diameter of 4-8 µm. Sphaeraphides are large (about 30-35 µm in diameter) occurring singly in parenchyma (Fig 4D). Rarely, oval sclereids also are seen. Cortex is delimited outside by thin walled epiblema consisting of thin-walled square cells (25 x25 µm).

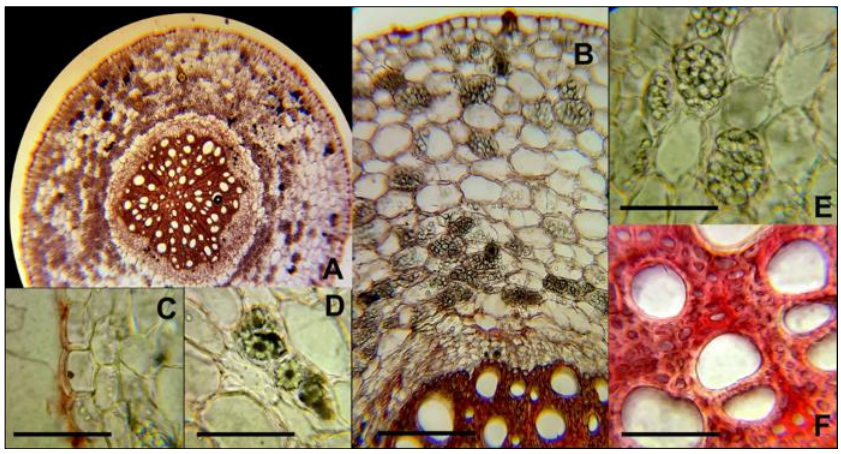

Fig 4: A. View of tranverse section of root showing a tetrarch stele. B. Phloem surrounding the central xylem. C. Endodermis showing yellow colored suberin. D. Sphaeraphides in cortex. E. Starch grains in parenchymatous cells of cortex. F. Large xylem vessels interspersed with tracheids. Scale bar: 400 µ (B), and 100µ (C-F)

DNA sequencing

The result indicated that, the intact amplified rubisco gene was of 520 base pairs and was obtained. The individual nucleotide peaks are shown in the electropherogram with its sequence as shown below in Figures 5 and 6.

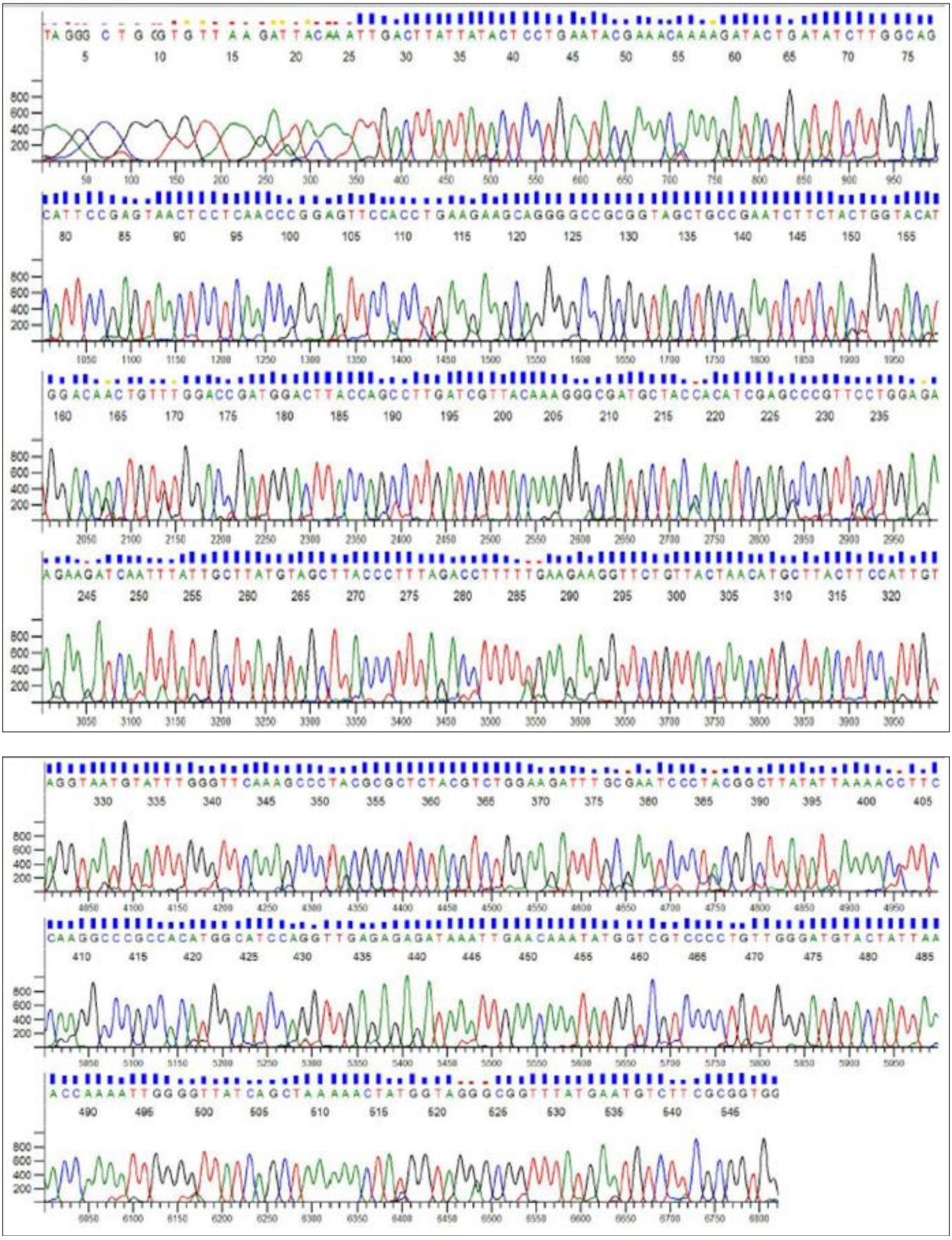

Fig 5: Electropherogram of Forward sequence of DNA in *V. indicum*

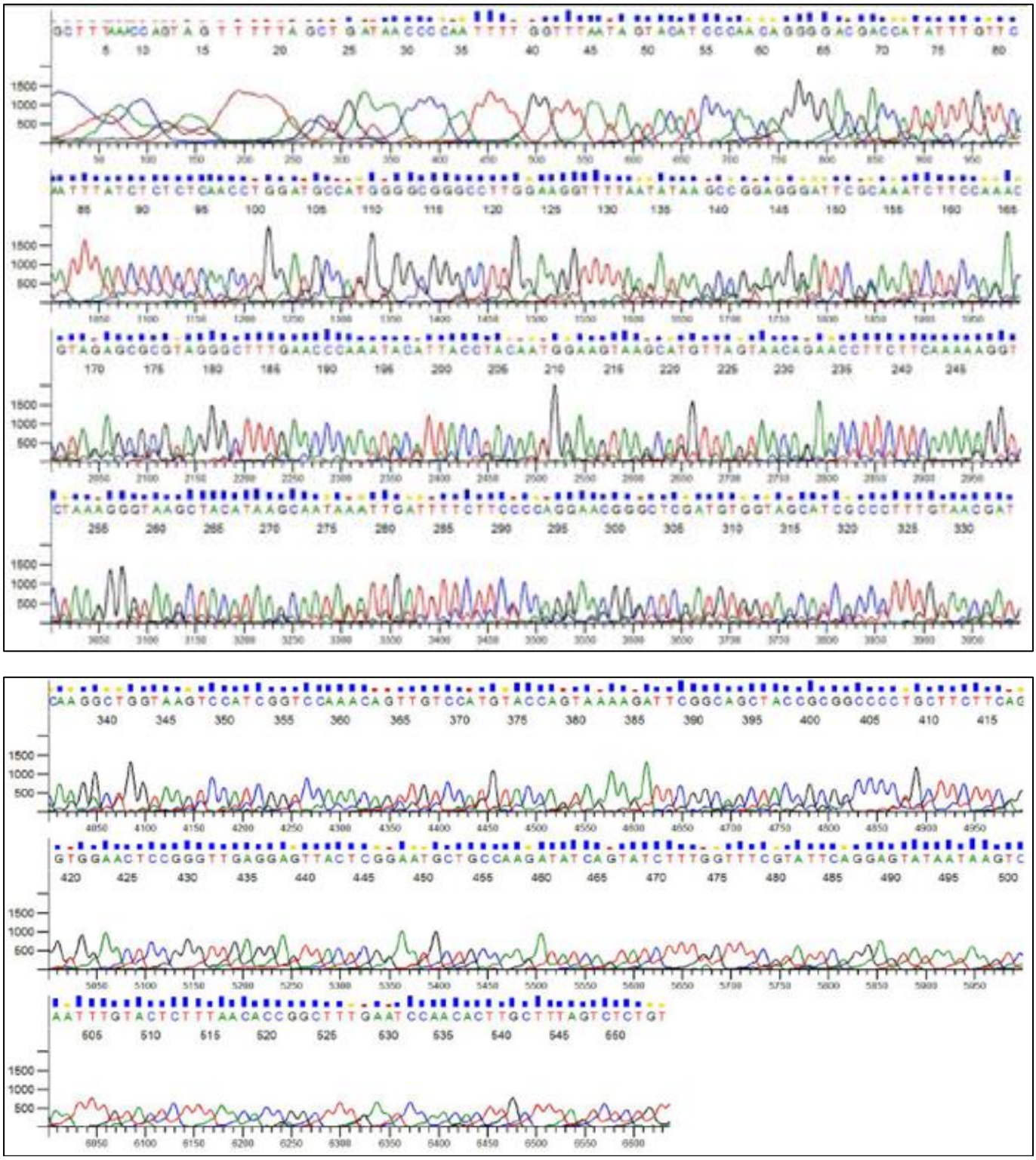

Fig 6: Electropherogram of Reverse sequence of DNA in *V. indicum*

Based on the electropherograms both the sequences have been interpreted as:

Forward sequence

TAGGGCTGGGTGTTAAGATTACAAATTGACTTATTAT
ACTCCTGAATACGAAACAAAAGATACTGATATCTTG
GCAGCATTCCGAGTAACTCCTCAACCCGGAGTTCCA
CCTGAAGAAGCAGGGGCCGCGGTAGCTGCCGAATCT
TCTACTGGTACATGGACAACTGTTTGGACCGATGGA
CTTACCAGCCTTGATCGTTACAAAGGGCGATGCTAC
CACATCGAGCCCGTTCCTGGAGAAGAAGATCAATTT
ATTGCTTATGTAGCTTACCCTTTAGACCTTTTTGAAG
AAGGTTCTGTTACTAACATGCTTACTTCCATTGTAGG
TAATGTATTTGGGTTCAAAGCCCTACGCGCTCTACGT
CTGGAAGATTTGCGAATCCCTACGGCTTATATTAAA
ACCTTCCAAGGCCCGCCACATGGCATCCAGGTTGAG
AGAGATAAATTGAACAAATATGGTCGTCCCCTGTTG
GGATGTACTATTAAACCAAAATTGGGGTTATCAGCT
AAAAACTATGGTAGGGCGGTTTATGAATGTCTTCGC
GGTGG.

Reverse sequence

GCTTTAAACCAGTAGTTTTTAGCTGATAACCCCAATT
TTGGTTTAATAGTACATCCCAACAGGGGACGACCAT
ATTTGTTCAATTTATCTCTCTCAACCTGGATGCCATG
GGGCGGGCCTTGGAAGGTTTTAATATAAGCCGGAGG
GATTCGCAAATCTTCCAAACGTAGAGCGCGTAGGGC

TTTGAACCCAAATACATTACCTACAATGGAAGTAAG
CATGTTAGTAACAGAACCTTCTTCAAAAAGGTCTAA
AGGGTAAGCTACATAAGCAATAAATTGATTTTCTTC
CCCAGGAACGGGCTCGATGTGGTAGCATCGCCCTTT
GTAACGATCAAGGCTGGTAAGTCCATCGGTCCAAAC
AGTTGTCCATGTACCAGTAAAAGATTCGGCAGCTAC
CGCGGCCCCTGCTTCTTCAGGTGGAACTCCGGGTTG
AGGAGTTACTCGGAATGCTGCCAAGATATCAGTATC
TTTGGTTTCGTATTCAGGAGTATAATAAGTCAATTTG
TACTCTTTAACACCGGCTTTGAATCCAACACTTGCTT
TAGTCTCTGT.

Confirmation of species

The sequence was submitted to NCBI and MT748762 accession no. was obtained. Additionally, NCBI BLAST resulted in 99% of the homology to the *Tylophora asthmatica* (Figure 7), suggesting the molecular confirmation of the species.

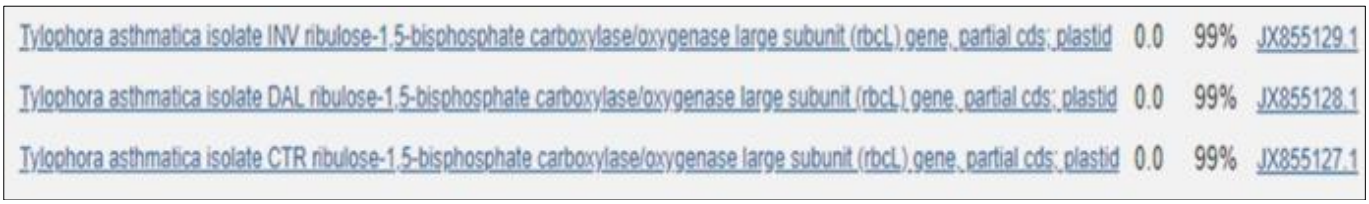

Fig 7: Species confirmation using BLAST homology model of NCBI database

Conclusion

The values calculated during the micromorphological studies can be used for quick analysis of the identity of the plant. The transverse sections of leaf, stem and root yielded key characters that can be used for correct identification of the plant, as well as its differentiation from other species.

The DNA sequence obtained can be used as an identification parameter for *Tylophora asthmatica*. This has helped in correctly identifying the plant species as there is huge morphological robustness in various similar species of same family. Thus, with the help of sequence, it is proved that the species is *Vincetoxicum indicum* belonging to family Apocynaceae of angiosperms.

References

1. Daniel M, Mammen D. Analytical Methods for Medicinal Plants and Economic Botany. Jodhpur, India: Scientific Publishers; c2016.
2. Malathi R, Gomez MP. Hepatoprotective effect of methanolic leaves extracts of Tylophora asthmatica against paracetamol-induced liver damage in rats. J Pharmacol Toxicol. 2007;2:737–742. https://doi.org/10.3923/jpt.2007.737.742
3. Jahan N, Khatoon R, Shahzad A, Shahid M, Ahmad S. Comparison of antibacterial activity of parent plant of Tylophora indica Merr. With its *in vitro* raised plant and leaf callus. Afr. J Biotechnol. 2013;12:4891–4896. https://www.cabidigitallibrary.org/doi/full/10.5555/20133312202
4. Raut S, Raut S, Ghadai A. Phytoceutical evaluation and antimicrobial properties of Eclipta alba and Tylophora indica. Int. J Microbiol. Res. 2012;4:227–230. http://dx.doi.org/10.9735/0975-5276.4.5.227-230.
5. Ravikumar A, Abbulu K. Evaluation of anti-inflammatory activity of Calotropis gigantean, Tylophora indica and Saecostemma secomone. Int Res J Pharmaceut Appl. Sci. 2011;1:34–42.
6. Raj CD, Shabi MM, Brahatheeswaran D, Mahesh N. Anti-inflammatory activity of Tylophora indica in albino rats. J Pharmacol Toxicol. 2006;1:490–492. https://doi.org/10.3923/jpt.2006.490.492
7. Patel NJ, Gujarati VB, Gouda TS, Rao NV, Nandakumar K, Shantakumar SM. Antidiarrhoeal activity of alcoholic and aqueous extracts of roots of Tylophora indica (Wight and Arn.) in rodents. Pharmacology online. 2006;1:19-29.
8. Mohammed Basheeruddin AS, Kapoor MS, Saifulla K. Effect of methanolic extract of Tylophora indica L. leaves on lipid profile in rats. J Pharm Res. 2009;8:56–60. https://dx.doi.org/10.18579/jpcrkc/2009/8/1/79792
9. Saraswati S, Kanaujia PK, Kumar S, Kumar R, Alhaider AA. Tylophorine, a phenanthraindolizidine alkaloid isolated from Tylophora indica exerts antiangiogenic and antitumor activity by targeting vascular endothelial growth factor receptor 2–mediated angiogenesis. Mol. Canc. 2013;12:01-16. https://doi.org/10.1186/1476-4598-12-82
10. Pratama NP, Wulandari S, Nugroho AE, Fakhrudin N, Astuti P, Sudarsono. Tylophorine abrogates G2/M arrest induced by doxorubicin and promotes increased apoptosis in T47D breast cancer cells. Asian Pac J Cancer Prev. 2019;19:3065–3069.
11. Pratheesh KV, Shine VJ, Emima J, Renju GL, Rajesh R. Study on the anticancer activity of Tylophora indica leaf extracts on human colorectal cancer cells. Int. J Pharmacogn Phytochem Res. 2014;6:355-361.
12. Gao W, Lam W, Zhong S, Kaczmarek C, Baker DC, Cheng Y. Novel mode of action of tylophorine analogs as antitumor compounds. Canc. Res. 2004;64:678–688. https://doi.org/10.1158/0008-5472.can-03-1904
13. Wu C, Yang C, Lee Y, Chuang T, Wu P, Chao Y, Lee S. Tylophorine arrests carcinoma cells at G1 phase by downregulating cyclin A2 expression. Biochem Biophys Res. Commun. 2009;386:140–145. https://doi.org/10.1016/j.bbrc.2009.05.138
14. Johansen DA. Plant Microtechnique. New York: McGraw Hill; c1940.
15. Wallis TE. Textbook of Pharmacognosy. 5th edition. London: J. and A. Churchill; c1957.
16. Ahmad SM, Ganaie MM, Qazi PH, Verma V, Basir SF, Qazi GN. Rapid DNA isolation protocol for angiospermic plants. Bulg J Plant Physiol. 2004;30:25-33. https://www.scirp.org/reference/referencespapers?referenceid=1698910
17. Healey A, Furtado A, Cooper T, Henry RJ. A simple method for extracting next-generation sequencing quality genomic DNA from recalcitrant plant species. Plant Methods. 2014;10:21. https://plantmethods.biomedcentral.com/articles/10.1186/1746-4811-10-21

18. Pathak A, Dwivedi M, Laddha N, Begum R, Joshi A. DNA isolation from fresh leaf tissue of Tylophora indica and Bacopa monnieri. Env. Exp. Bio. 2013;11:69-71.
19. Sika KC, Kefala T, Adoukonou-Sagbabja H, Ahotan L, Saidou A, Baba-Moussa L, *et al*. A simple and efficient genomic DNA extraction protocol for large scale genetic analysis of plant biological systems. Plant Gene. 2015;1:43-45. http://dx.doi.org/10.1016/j.plgene.2015.03.001